

Numerical Study of Plasma Transport Equations

Mohamed El Haim¹, Mohamed Atounti², and Mohamed El Bojaddaini³

¹Department of Civil Engineering, Energetic and Environment, Team of Modeling, Optimization and Structure Dynamics in Civil Engineering, Laboratory of Applied Sciences, Abdelmalek Essaadi University, National School of Applied Sciences, Al Hoceima, Morocco

²Department of Mathematics and Computer Sciences, Laboratory of Applied Mathematics and Information Systems, Mohammed Ist University, Multidisciplinary Faculty, Nador, Morocco

³Department of Physics, Laboratory of Physics of Matter and Radiation, Mohammed Ist University, Faculty of Sciences, Oujda, Morocco

Copyright © 2019 ISSR Journals. This is an open access article distributed under the ***Creative Commons Attribution License***, which permits unrestricted use, distribution, and reproduction in any medium, provided the original work is properly cited.

ABSTRACT: This paper presents the numerical method used to solve the nonlinear plasma fluid equations. We have developed a fluid plasma model for a microwave plasma CVD reactor used for diamond thin film deposition. This model solves the electron and ion continuity equations, momentum transport equation and the Poisson's equation. In these equations we have the problem of non-linearity which is solved using the Newton's method. From these equations, the unknowns computed are electron and ion densities (n_e, n_i), and plasma potential (ψ). Then the impacts of the hydrogen pressure and microwave power density have been studied. Simulation results show a strong effect of these parameters on the species densities distribution in the plasma.

KEYWORDS: Numerical method, fluid plasma model, microwave plasma CVD reactor, Newton Raphson's method, Finite difference method.

1 INTRODUCTION

Deposition reactors and surface treatment assisted by plasma are currently used in many industries. Different types of plasmas used in these reactors, those created by microwave discharges. The MPACVD (Microwave Plasma Chemical Vapor Deposition) reactor contains a cylindrical resonant cavity. The microwave plasma is coupled with an electromagnetic wave at a frequency of excitation 2.45 GHz. Thus, interactions between plasma and electromagnetic waves are governed simultaneously by the equations of motion of particles and Maxwell's equations.

However, discharge plasma has physicochemical phenomena very complex and strongly coupled. Further, it is difficult to experimentally observe physical quantities of plasmas inside the reactors. Therefore, the numerical simulation of microwave plasma is a necessity [1] to understand the plasma behavior inside the reactor, and to improve the knowledge for deposition or etching by means of plasma technology.

In this present work we try to expose a numerical simulation of a pure hydrogen discharge characteristics, using a fluid plasma model. We chose the hydrogen plasma example because diamond film deposition processes often consist of high percentages of hydrogen in the discharge [2].

To study the physicochemical phenomena of plasma we can use some average values which define in a less complete way the state of the system. These sizes are macroscopic parameters defined in every point of the plasma such as: Electron density, velocity, pressure tensor, tensor of the flow quantity of heat.

This description is the same kind as that which is used in hydrodynamics for the study of ordinary fluid. The quantities obtained in this way are governed by the laws of conservation of base such as: conservation of mass, momentum and energy.

The numerical solution of these equations makes the problem more difficult. There is a hierarchy of physical models corresponding to different degrees of approximation of phenomena such as: Fluid models [3], [4], [5], particle-in-cell/Monte Carlo (PIC/MC) models [6], [7] and hybrid models [8], [9]. All these modeling approaches have their specific advantages and limitations, and therefore, the choice of the model is often dictated by the gas discharge and conditions under study [10]. The fluid plasma model are presented and developed in the following sections.

2 FLUID MODEL FOR A MICROWAVE PLASMA

The simulation of plasma processes can be based generally on two major approaches. One is the particle approach, which is carried out using a particle simulation technique that treats the plasma as a combination of particles (electron, ion, neutral).

The other approach is the fluid method, which treats the plasma as a fluid and solves the equations obtained from the moments of the Boltzmann transport equation [11].

However, this model can treat the equations of continuity, transfer momentum and energy. These equations are similar to those of the mechanics of fluids with different levels of force terms and collisions terms.

The Boltzmann equation (BE) is a fundamental equation describing the transport of an ensemble of particles. It is given by the following form [11]:

$$\left(\frac{\partial}{\partial t} + \vec{v} \cdot \vec{\nabla} + \frac{\vec{F}}{m} \cdot \vec{\nabla}_v \right) f(\vec{r}, \vec{v}, t) = \left(\frac{\partial f(\vec{r}, \vec{v}, t)}{\partial t} \right)_{coll} \tag{1}$$

Here, $f(\vec{r}, \vec{v}, t)$ is the distribution function, \vec{r} denotes the spatial position, \vec{v} denotes the velocity, and t denotes the time. m is the mass of the particle, \vec{F} denotes external forces, and the term on the right side of the eq.(1) represents the collision term of the Boltzmann equation, is the so-called collision integral which accounts for changes of the electron velocity distribution function because of collisions electrons undergo mainly with neutrals but also with other electrons and ions [11].

Eq.(1) is a partial integro-differential equation in seven dimensions (three in space, three in velocity and time), and as such is extremely difficult to solve [11].

The fluid model of plasma, reducing the complexities in the kinetic description, is based on partial differential equations which describe the macroscopic quantities such as: density, flux, average velocity, pressure, temperature. Then if we take a velocity moments in the Boltzmann equation, The fluid equations are obtained [12].

Zero moment of the Boltzmann equation $\int_{-\infty}^{+\infty} (BE) d^3v$ yields continuity equation for the particle density like:

$$\frac{\partial n}{\partial t} + \vec{\nabla} \cdot (n \vec{u}) = \int_{-\infty}^{+\infty} \left(\frac{\partial f}{\partial t} \right)_{coll} d^3v \tag{2}$$

Here, the particle density n and the average velocity \vec{u} are defined as:

$$n = \int_{-\infty}^{+\infty} f d^3v$$

$$\vec{u} = \frac{1}{n} \int_{-\infty}^{+\infty} \vec{v} f d^3v$$

The source term on the right side of the continuity equation corresponds to the collision term of the Boltzmann equation.

First moment of the Boltzmann equation $(m \int_{-\infty}^{+\infty} \vec{v} (BE) d^3v)$ gives the momentum transport equation called also equation of motion such as:

$$m n \frac{\partial \vec{u}}{\partial t} + m n (\vec{u} \cdot \nabla) \vec{u} + \nabla \vec{P} - n q (\vec{E} + \vec{u} \times \vec{B}) = m \int_{-\infty}^{+\infty} (\vec{v} - \vec{u}) \left(\frac{\partial f}{\partial t} \right)_{coll} d^3v \tag{3}$$

\vec{E} and \vec{B} are the electric and magnetic fields, respectively.

Similarly, the energy equation can be found as second moment of the Boltzmann equation:

$(\frac{1}{2} m \int_{-\infty}^{+\infty} v^2 (BE) d^3v)$ as:

$$\frac{1}{\gamma-1} \left(\frac{\partial p}{\partial t} + \nabla \cdot (p \vec{u}) \right) + (\vec{P} \cdot \nabla) \vec{u} + \nabla \cdot \vec{Q} = \frac{1}{2} m \int_{-\infty}^{+\infty} (\vec{v} - \vec{u})^2 \left(\frac{\partial f}{\partial t} \right)_{coll} d^3v \quad (4)$$

\vec{P} is the pressure tensor as $\vec{P} = m \int_{-\infty}^{+\infty} (\vec{v} - \vec{u})(\vec{v} - \vec{u}) f d^3v$, and $P_{ij} = p \delta_{ij}$ defines scalar pressure p . γ is the ratio of specific heats.

This simulation consists of the particle and momentum equations for electrons and ions, which are combined with the Poisson's equation.

In the steady state, the governing equations used in this study are given by [2]:

$$\nabla^2 \psi = \frac{e}{\epsilon} (n_e - n_i) \quad (5)$$

$$\vec{\nabla} \cdot \vec{J}_e = n_e n_n k_{ion} - \alpha_r n_i n_e \quad (6)$$

$$\vec{\nabla} \cdot \vec{J}_i = n_e n_n k_{ion} - \alpha_r n_i n_e \quad (7)$$

$$\vec{J}_e = -n_e \mu_e \vec{E} - D_e \vec{\nabla} n_e \quad (8)$$

$$\vec{J}_i = n_i \mu_i \vec{E} - D_i \vec{\nabla} n_i \quad (9)$$

Equation (5) represents the Poisson's equation, which gives the electric interaction between electrons and ions [13], where ψ is the electric potential.

The electric field \vec{E} is derived from a scalar potential, ψ , by:

$$\vec{E} = -\vec{\nabla} \psi \quad (10)$$

Equations (6) and (7) represent the electron and ion continuity equations, respectively. Other equations (8) and (9) represent the momentum balances for electrons and ions, respectively.

The drift diffusion approximation reduces the number of partial differential equations included in model by the use of the algebraic expression for particle flux (Equations (8) and (9)) instead of full equation of motion [12], [14].

In the above equations, n_e and n_i are the electron and ion densities, respectively; \vec{J}_e and \vec{J}_i are the electron and ion fluxes, respectively; k_{ion} is the inelastic rate constant for ionization; and α_r is the recombination rate constant ($\alpha_r = 1.0 \times 10^{-13} m^3 \cdot s^{-1}$); $D_{e,i}$ and $\mu_{e,i}$ are the electron and ion diffusivities and mobilities, respectively.

3 MODEL FORMULATION IN CYLINDRICAL COORDINATES

The reactor has a cylindrical geometry. Then we develop the fluid model equations in cylindrical coordinates as:

POISSON'S EQUATION :

$$\frac{\partial^2 \psi}{\partial r^2} + \frac{1}{r} \frac{\partial \psi}{\partial r} + \frac{\partial^2 \psi}{\partial z^2} = \frac{e}{\epsilon_0} (n_e - n_i) \quad (11)$$

And to calculate the components of the electric field, the following two equations are used:

$$E_r = -\frac{\partial \psi}{\partial r}; E_z = -\frac{\partial \psi}{\partial z} \quad (12)$$

CONTINUITY EQUATION FOR THE ELECTRONS :

The two equations (6) and (8) were combined to give the continuity equation for electrons as:

$$\begin{aligned} -D_e \left[\frac{\partial^2 n_e}{\partial r^2} + \frac{1}{r} \frac{\partial n_e}{\partial r} + \frac{\partial^2 n_e}{\partial z^2} \right] + \mu_e \left[\frac{\partial \psi}{\partial r} \cdot \frac{\partial n_e}{\partial r} + \frac{\partial \psi}{\partial z} \cdot \frac{\partial n_e}{\partial z} \right] \\ + \mu_e \left[\frac{\partial^2 \psi}{\partial r^2} + \frac{1}{r} \frac{\partial \psi}{\partial r} + \frac{\partial^2 \psi}{\partial z^2} \right] n_e + \alpha_r n_i n_e - k_{ion} n_n n_e = 0 \end{aligned} \quad (13)$$

CONTINUITY EQUATION FOR THE IONS :

On the other hand, the two equations (7) and (9) were combined to give the continuity equation for ions as:

$$\begin{aligned} -D_i \left[\frac{\partial^2 n_i}{\partial r^2} + \frac{1}{r} \frac{\partial n_i}{\partial r} + \frac{\partial^2 n_i}{\partial z^2} \right] - \mu_i \left[\frac{\partial \psi}{\partial r} \cdot \frac{\partial n_i}{\partial r} + \frac{\partial \psi}{\partial z} \cdot \frac{\partial n_i}{\partial z} \right] \\ - \mu_i \left[\frac{\partial^2 \psi}{\partial r^2} + \frac{1}{r} \frac{\partial \psi}{\partial r} + \frac{\partial^2 \psi}{\partial z^2} \right] n_i + \alpha_r n_i n_e - k_{ion} n_n n_e = 0 \end{aligned} \quad (14)$$

4 DISCRETIZATION OF THE EQUATIONS IN 2D

We choose the symmetry along the axis (Oz) as shown in Fig. 1. And finite difference techniques are used to discretize the cylindrical coordinates form of equations (11) to (14) using in the centered scheme.

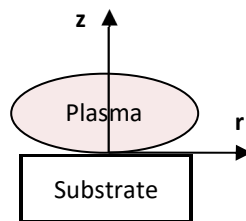


Fig. 1. Mark (O,r,z) corresponding to the symmetry of the reactor

Using a mesh size of the plasma medium along the two axes (or) and (oz) with steps Δr and Δz . In this discretization we take an uniform mesh when $\Delta r = \Delta z$.

DISCRETIZATION OF THE POISON'S EQUATION :

$$\begin{aligned} & \frac{\psi(i+1, j) - 2\psi(i, j) + \psi(i-1, j)}{(\Delta r)^2} + \frac{\psi(i+1, j) - \psi(i-1, j)}{2i(\Delta r)^2} \\ & + \frac{\psi(i, j+1) - 2\psi(i, j) + \psi(i, j-1)}{(\Delta z)^2} - \frac{e}{\epsilon_0} [n_e(i, j) - n_i(i, j)] = 0 \end{aligned} \quad (15)$$

CONTINUITY EQUATION FOR ELECTRONS DISCRETIZED:

$$\begin{aligned} & -D_e \left[\frac{n_e(i+1, j) - 2n_e(i, j) + n_e(i-1, j)}{(\Delta r)^2} + \frac{n_e(i+1, j) - n_e(i-1, j)}{2i(\Delta r)^2} \right] \\ & -D_e \left[\frac{n_e(i, j+1) - 2n_e(i, j) + n_e(i, j-1)}{(\Delta z)^2} \right] \\ & + \mu_e \left[\frac{\psi(i+1, j) - \psi(i-1, j)}{2(\Delta r)} \cdot \frac{n_e(i+1, j) - n_e(i-1, j)}{2(\Delta r)} \right] \\ & + \mu_e \left[\frac{\psi(i, j+1) - \psi(i, j-1)}{2(\Delta z)} \cdot \frac{n_e(i, j+1) - n_e(i, j-1)}{2(\Delta z)} \right] \\ & + \mu_e \left[\frac{\psi(i+1, j) - 2\psi(i, j) + \psi(i-1, j)}{(\Delta r)^2} + \frac{\psi(i+1, j) - \psi(i-1, j)}{2i(\Delta r)^2} \right] \cdot n_e(i, j) \\ & + \mu_e \left[\frac{\psi(i, j+1) - 2\psi(i, j) + \psi(i, j-1)}{(\Delta z)^2} \right] \cdot n_e(i, j) \\ & -n_n k_{ion} n_e(i, j) + \alpha_r n_i(i, j) n_e(i, j) = 0 \end{aligned} \quad (16)$$

CONTINUITY EQUATION FOR IONS DISCRETIZED:

$$\begin{aligned} & -D_i \left[\frac{n_i(i+1, j) - 2n_i(i, j) + n_i(i-1, j)}{(\Delta r)^2} + \frac{n_i(i+1, j) - n_i(i-1, j)}{2i(\Delta r)^2} \right] \\ & -D_i \left[\frac{n_i(i, j+1) - 2n_i(i, j) + n_i(i, j-1)}{(\Delta z)^2} \right] \\ & -\mu_i \left[\frac{\psi(i+1, j) - \psi(i-1, j)}{2(\Delta r)} \cdot \frac{n_i(i+1, j) - n_i(i-1, j)}{2(\Delta r)} \right] \\ & -\mu_i \left[\frac{\psi(i, j+1) - \psi(i, j-1)}{2(\Delta z)} \cdot \frac{n_i(i, j+1) - n_i(i, j-1)}{2(\Delta z)} \right] \\ & -\mu_i \left[\frac{\psi(i+1, j) - 2\psi(i, j) + \psi(i-1, j)}{(\Delta r)^2} + \frac{\psi(i+1, j) - \psi(i-1, j)}{2i(\Delta r)^2} \right] \cdot n_i(i, j) \\ & -\mu_i \left[\frac{\psi(i, j+1) - 2\psi(i, j) + \psi(i, j-1)}{(\Delta z)^2} \right] \cdot n_i(i, j) \\ & -n_n k_{ion} n_e(i, j) + \alpha_r n_i(i, j) n_e(i, j) = 0 \end{aligned} \quad (17)$$

In these above equations i and j denote the grid indices in the r and z directions respectively, such as $1 \leq i \leq (L - 1)$ and $1 \leq j \leq (M - 1)$ where $r = L \cdot \Delta r$, $z = 0$ (substrat) and $z = M \cdot \Delta z$ denote the edges of the plasma midium in the r and z directions respectively.

To resolve the coupled equations (15), (16) and (17) we need the boundary conditions at the substrate and the edges of the plasma volume:

- For the electron density : $n_e(i, 0) = n_e(i, M) = n_e(L, j) = 0$
- For the ion density : $n_i(i, 0) = n_i(i, M) = n_i(L, j) = 0$
- For the electric potential : $\Psi(i, 0) = \Psi(i, M) = \Psi(L, j) = 0$

(18)

And for the centerline where $r=0$ the following condition is used:

$$\left(\frac{\partial n_e}{\partial r}\right)_{(0,j)} = \left(\frac{\partial n_i}{\partial r}\right)_{(0,j)} = \left(\frac{\partial \Psi}{\partial r}\right)_{(0,j)} \quad (19)$$

5 RATE AND TRANSPORT PARAMETERS FOR HYDROGEN GAS

The different rate and parameters for the hydrogen gas encountered in equations (16) and (17) as k_{ion} , D_e , D_i , μ_e , μ_i , α_r , and n_n are determined by the following relations such as the Arrhenius relationship [2], [15]:

$$k_{ion} = A_{ion} \exp\left(\frac{-\varepsilon_{ion}}{K_B T_e}\right) \quad (20)$$

ε_{ion} denotes the threshold energy for H₂ molecule ionization ($\varepsilon_{ion} = 15.4 \text{ eV}$);

T_e is the electron temperature;

K_B is the Boltzmann constant;

And A_{ion} is the pre-exponential factor which is obtained by approximating the rate constant data at low electron temperatures to this relationship [15] ($A_{ion} = 1.0 \times 10^{-14} \text{ m}^3 \cdot \text{s}^{-1}$).

First, determining the collision frequency for electron-H₂ molecule momentum transfer by applying the relation [2]:

$$v_{en} = 1.44 \times 10^{12} \times \frac{P_r(\text{Torr})}{T_n(\text{K})} \quad (21)$$

T_n is the neutral temperature which can be calculated by the translational temperature of H₂ gas given by [2]:

$$T_n(\text{K}) = 228.6 + 374.3 \times P_{inc}(\text{kW}) + 16.5 \times P_r(\text{Torr}) \pm 94.2 \quad (22)$$

Where P_{inc} the incident is power in (kW) and P_r is the pressure into the reactor cavity in (Torr). And in this study, it is assumed that 100% of the microwave power coupled into the reactor is absorbed by the plasma.

After we can determine the electron diffusivity and mobility respectively as [15]:

$$D_e = \frac{K_B T_e}{m_e v_{en}} \quad (23)$$

$$\mu_e = \frac{e}{m_e v_{en}} \quad (24)$$

e is the elementary charge and m_e is the electron mass.

In other hand we deduce the neutral density n_n by applying the relation between transport parameters as [15]:

$$D_e \cdot n_n = 5.0 \times 10^{23} \text{ m}^{-1} \cdot \text{s}^{-1} \quad (25)$$

Then we can easily deduce the parameters μ_i and D_i by applying the following relationships [15]:

$$\mu_i \cdot n_n = 3.5 \times 10^{22} \text{ m}^{-1} \cdot \text{V}^{-1} \cdot \text{s}^{-1} \tag{26}$$

Finally, we can even calculate the volume of plasma depending on the incident power and pressure given by [2]:

$$V(\text{cm}^3) = 449.7 + 116.2 \times P_{inc}(\text{kW}) - 18.1 \times P_r(\text{Torr}) + 57.1 \times P_{inc}^2(\text{kW}) + 0.25 \times P_r^2(\text{Torr}) - 5.4 \times P_r(\text{Torr}) \times P_{inc}(\text{kW}) \pm 15.4 \tag{27}$$

6 APPLICATION OF THE NEWTON-RAPHSON METHOD

Newton’s method is used to solve the nonlinear discretized equations (16) and (17) to obtain plasma electric potential (Ψ), electron density (n_e), and ion density (n_i).

In this section we will discuss the simplest multidimensional root finding method, Newton-Raphson. If we have a sufficiently good initial guess, this method gives us a very efficient means of converging to a root.

Our problem gives N functional relations to be zeroed, involving variables x_i where:

$$i = 1, 2, \dots, (L + 1)(M + 1), [(L + 1)(M + 1)] + 1, \dots, 2(L + 1)(M + 1), [2(L + 1)(M + 1)] + 1, \dots, N.$$

We set: $N = 3(L + 1)(M + 1)$.

So the N functional relations are written as:

$$F_i(x_1, x_2, x_3, \dots, x_N) = 0 \text{ where } i = 1, 2, 3, \dots, N \tag{28}$$

We let x denote the entire vector of values x_i and F denote the entire vector of function F_i . In the neighborhood of x , each of the functions can be expanded in Taylor series [16]

$$F_i(x + \delta x) = F_i(x) + \sum_{j=1}^N \frac{\partial F_i}{\partial x_j} \delta x_j + 0(\delta x^2) \tag{29}$$

It must resonate step by step as follows:

- Write the N functional relations: $F_i(x) = 0$
- Calculate the elements of the Jacobian matrix J : $J_{ij} = \frac{\partial F_i}{\partial x_j}$ (30)
- Calculate the coordinates of the second member vector: $B_i = -F_i(x)$ (31)
- Write the Newton function as : $x_{i+1} = x_i - \frac{F_i(x)}{\frac{\partial F_i(x)}{\partial x_i}}$ (32)
- Choose an initial value : x_0
- While $\|x_{i+1} - x_i\| \geq \epsilon$ and the number of iterations is less than N_{max} , calculate the new value of x_i starting with x_1
- If $\|x_{i+1} - x_i\| < \epsilon$ then Newton's method converges else it doesn't converge.

Fig. 2 shows the organigram of Newton's method followed:

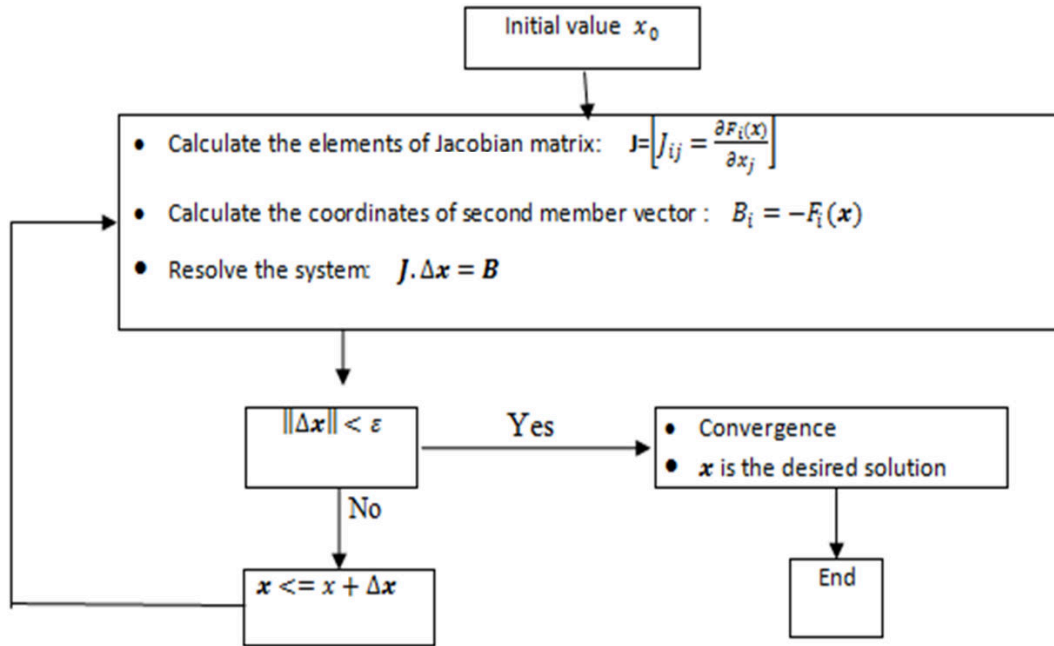


Fig. 2. Organigram of the Newton-Raphson method

7 NUMERICAL RESULTS AND DISCUSSION

The simulation results shown in this section were all performed in the geometry presented in the Fig.1. The main input parameters for this numerical study include the pressure and microwave power.

In the fig.3 and fig.4 we present the spatial distribution of plasma density related of a given microwave power density. The results show that the plasma density is maximal in the plasma volume near the center of the discharge (r=0cm), and decreases in the edges and near the substrate region. We see also that the maximum electron density increases with increased power density [16].

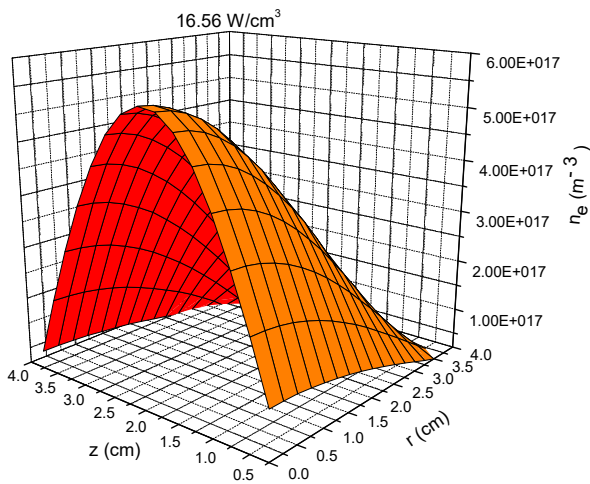


Fig. 3. Two-dimensional distribution of plasma density at a power density of 15.56 W/cm³

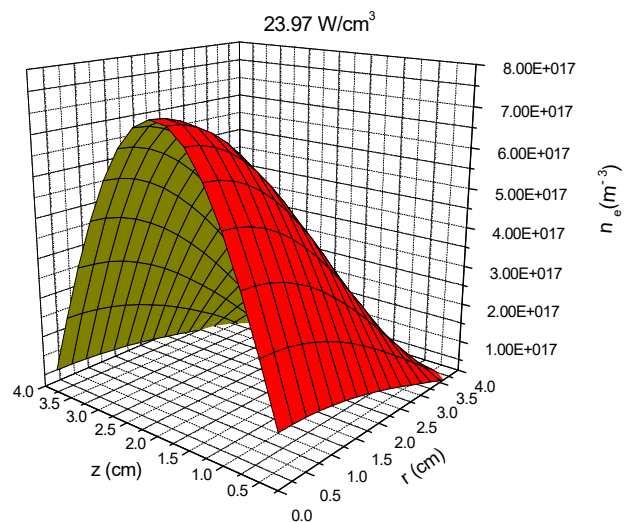


Fig. 4. Two-dimensional distribution of plasma density at a power density of 23.97 W/cm³

By increasing simultaneously power and gas pressure keeping constant the plasma volume, the evolution of axial and radial profiles of electron density, for different power densities, is also calculated and presented in the following figures.

Fig.5 indicate the evolution of electron density along the axial direction in the hydrogen discharge at a fixed radial position $r=0\text{cm}$, for different power densities, where the substrate is situated at the position $z=0\text{cm}$. As shown, the electron density increases at the first, reaches it is maximum at the center of the discharge and then vanishes near the edge of the plasma [17].

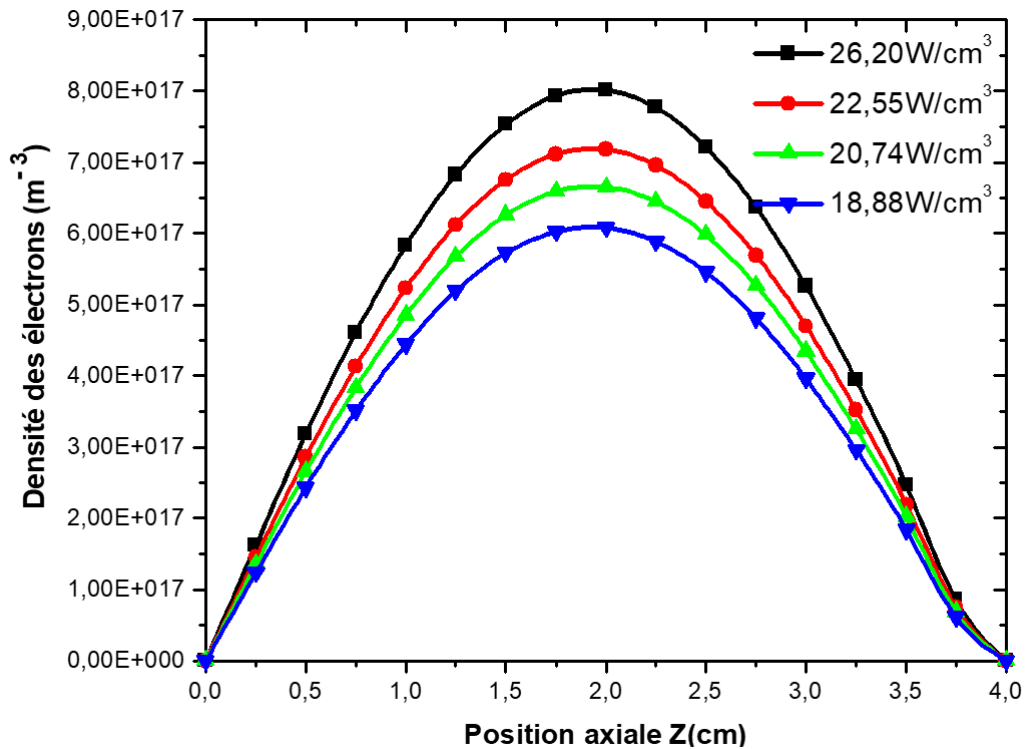


Fig. 5. Axial profile of electron density for different power densities at $r = 0 \text{ cm}$

The radial profile of electron density in the discharge for different power densities are shown in fig.6. We see that the electron density decreases from its maximum values at the center to a minimum value at the edge of the plasma volume.

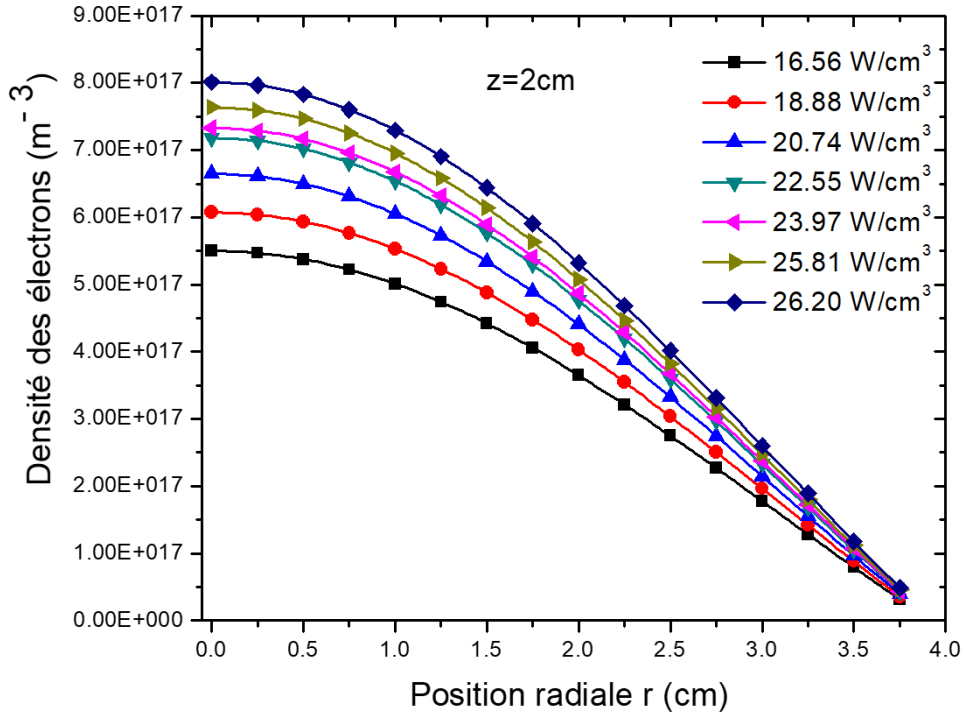


Fig. 6. Radial Profile of electron density for different power densities at $z=2\text{cm}$

The fig.7 shows the evolution of both ion and electron densities as a function of the pressure of the hydrogen gas within the reactor.

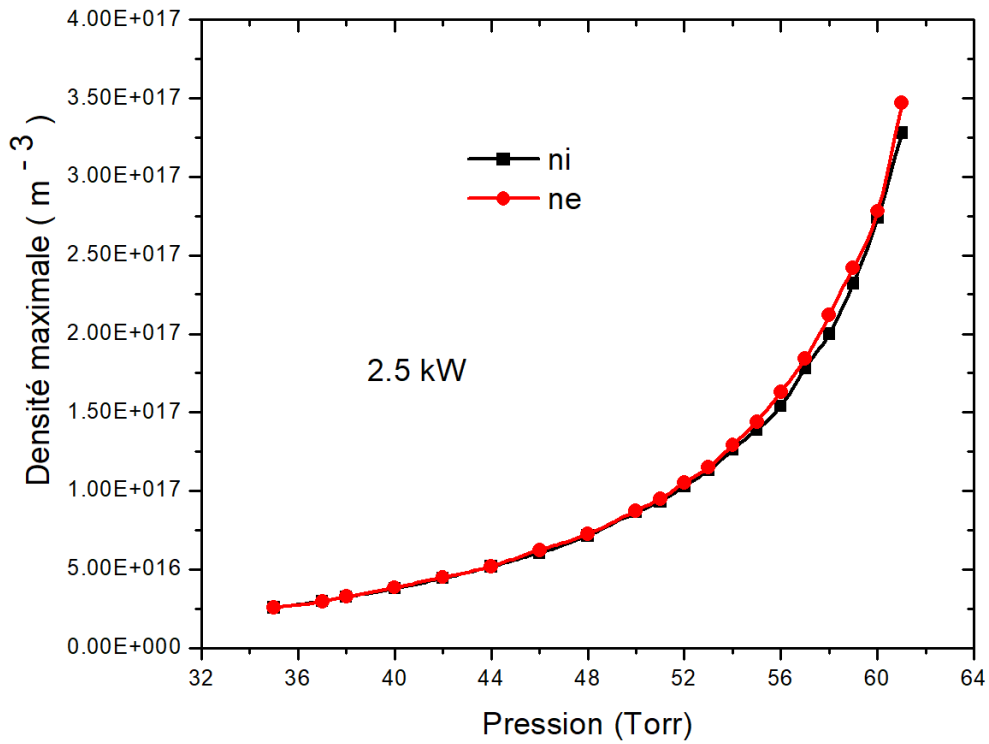


Fig. 7. Maximum densities of electrons and ions for incident power of 2.5kW

We see that the maximum values of the electron and ion density increases with increasing gas pressure. And the maximum value of the electron density is almost the same as the ion density at a given pressure and power value.

8 CONCLUSION

In this paper, a fluid plasma model is presented to describe the hydrogen microwave plasma discharge characteristics by solving the electron and ion continuity equations, momentum transport equation and the Poisson's equation.

The Newton-Raphson method is applied in order to solve the nonlinear equations. We have focused on distributions of electrons number density to provide information on the characteristics of hydrogen plasma. In other hand we tried to compare the maximum electron density with the maximum ion density for different values of pressure and constant incident power.

The distribution of electrons density is obtained for various conditions of power and pressure. The simulations results show a strong effect of gas pressure and power density on the plasma density.

REFERENCES

- [1] M. Funer, C. Wild and P. Koidl: *Surface and Coatings Technology*, 116-119, 1999.
- [2] W. Tan, T. A. Grotjohn, *Diamond and Related Materials* vol. 4, pp. 1145-1154, 1995.
- [3] G. J. Nienhuis, W. J. Goedheer, *Plasma Sources Sci. Techn.*, 8, 295, 1999.
- [4] K. Bera, B. Farouk, Y. H. Lee, *Plasma Sources Sci. Tech.*, 10, 211, 2001.
- [5] D. Herrebout, A. Bogaerts, M. Yan, R. Gijbels, W. Goedheer and A. Vanhulsel, *Journal of Applied Physics*, 92, 2290 2002.
- [6] M. Yan, W. J. Goedheer, *IEEE Transactions on Plasma Science*, 27, 1399, 1999.
- [7] K. Nagayama, B. Farouk, Y. H. Lee, *IEEE Transactions on Plasma Science*, 26, 125, 1998.
- [8] A. Bogaerts, R. Gijbels, W. J. Goedheer, *J. Appl. Phys*, 78, 2233, 1995.
- [9] A. Bogaerts, R. Gijbels, W. Goedheer, *Anal. Chem.*, 68, 2296, 1996.
- [10] A. Bogaerts, E. Bultinck, M. Eckert, V. Georgieva, M. Mao, E. Neyts and L. Schwaederle, "Computer Modeling of Plasmas and Plasma-Surface Interactions", *Plasma Process. Polym.* 6, 295-307, 2009.
- [11] Demetre. J. Economou, "Modeling and Simulation of Plasma etching reactors for microelectronics", *Thin Solid Films* 365-348-367, 2000.
- [12] E. Havlickova, "Fluid Model of Plasma and Computational Methods for Solution", *WDS'06 Proceedings of contributed Papers, Part III*, 180-186, 2006.
- [13] P. Scheubert, P. Awakowicz, R. Schwefel and G. Wachutka, *Surface and Coatings Technology*, 142-144, 526-530, 2001.
- [14] M. Meyyappan and J. P. Kreskovsky, *J. Appl. Phys.* 68 (4), 15 August 1990.
- [15] M. Surendra; D. B. Graves and L. S. Plano, *J. Appl. Phys.* 71 (10), 15 May 1992.
- [16] M. El Haim, *Modélisation Numérique et Caractérisation des Décharges Micro-ondes : Application aux Réacteurs MPACVD*, Ph.D. dissertation, Mohammed 1st Univ, Oujda, Morocco, 2015.
- [17] M. El Bojaddaini, H. Chatei, M. Atounti, M. El Hammouti, and M. EL Haim, "Numerical Simulation of Plasma Characteristics using Fluid Model with Drift Diffusion Approximation", *Journal of Advanced Mathematical Studies*, Vol. 11, N^o. 2, 259-264, 2018.